Application of Polyurethane/Gamma-Irradiated Carbon Nanotubes Composites as Antifouling Coat

Hanan M. Eyssa,[1] **Dalia E. Abulyazied**,[2] **Mervat A. M. Abo-State**[3]
[1]*Radiation Chemistry Department, National Centre for Radiation Research and Technology (NCRRT), Egyptian Atomic Energy Authority, Nasr City, Cairo, Egypt*

[2]*Petrochemical Department, Polymer Laboratory, Egyptian Petroleum Research Institute, Nasr City, Cairo, Egypt*

[3]*Radiation Microbiology Department, National Centre for Radiation Research and Technology (NCRRT), Egyptian Atomic Energy Authority, Nasr City, Cairo, Egypt*

The aim of this study is to avoid or reduce the risks of biofouling of ship hulls, using polyurethane/γ-irradiated functionalized multiwall carbon nanotubes (PU/FMWCNT) nanocomposites as a coating for wood. These nanocomposites were characterized by Fourier transform infrared spectroscopy (FTIR) measurements, transmission electron microscopy (TEM), and field emission scanning electron microscopy (FESEM), and hardness, adhesion, and bending of the coated samples were examined. The antifouling ability of PU/γ-irradiated FMWCNTs was studied by using an algae test. FTIR proved the presence of COOH group on the surface of MWCNT, while the FESEM results showed good dispersion of FMWCNT in polyurethane matrix. Mechanical properties of the coated wooden samples were improved; the samples showed good hardness and very good adhesion, and reasonable flexural modulus. The antifouling property of the coatings showed that 0.1 and 0.2 wt% FMWCNTs immobilized on polyurethane composite and irradiated for 100 kGy, were the most efficient antifouling coat when immersed in *Chlorella vulgaris* microalgae. POLYM. COMPOS., 39:E1196–E1207, 2018.

INTRODUCTION

Marine biofouling is the accumulation or adsorption of micro- and macro-organisms on wet surfaces, which is a worldwide problem affecting aquatic industries. Biofouling can reduce the speed and maneuverability of ships, accelerate corrosion, and increase fuel consumption and increase the risk of mechanical failure [1]. To overcome this problem, specifically designed materials and coatings with the ability to remove biofouling are used.

Correspondence to: D. E. Abulyazied; e-mail: daliaelsawy@hotmail.com
DOI 10.1002/pc.24718
Published online in Wiley Online Library (wileyonlinelibrary.com).

Antifouling biocides were used several decades ago. However, they have been banned due to the toxic nature of certain types, such as tributyltin 22 and copper, which cause marine pollution [2]. Other approaches have thus been researched for development of biocide-free antifouling coatings, due to their huge impact on the environment. Biofouling occurs on four stages: first one is the formation of the conditions layer, second is the settlement of microorganisms, third is the colonization of algae spores and marine larva, and fourth is the attachment of large organisms [3, 4].

Besides the remarkable chemical stability and the mechanical, optical, thermal, and electrical properties of carbon nanotubes (CNTs), composites based on functionalized carbon nanotubes (FCNTs) are used as multifunctional coating material. For example, MWCNT-containing paints possess lower biofouling of ship hulls by discouraging attachment of algae, while barnacles [5] have gained much attention because of their improved properties; they are a possible alternative to environmentally hazardous biocide-containing paints.

Polyurethanes have been used in recent years in antifouling coatings. Most research studies have focused on organic fluorine- and silicone-modified polyurethane where silicone and fluorine provide lower surface energy for antifouling [6–8]. Contrarily, research studies conducted to determine the antifouling properties of polyurethane alone are limited. It is expected that the surface properties of polyurethane coatings will be changed in seawater due to chain segment motion occurring upon immersion, probably changing the antifouling performance of the polyurethane coating. Polyurethane can be easily produced by controlling the chemical structure and content of the soft and hard segments, which are the basic components of polyurethane. Moreover, combining polyurethane with nanomaterials offers outstanding antifouling ability and excellent mechanical properties and

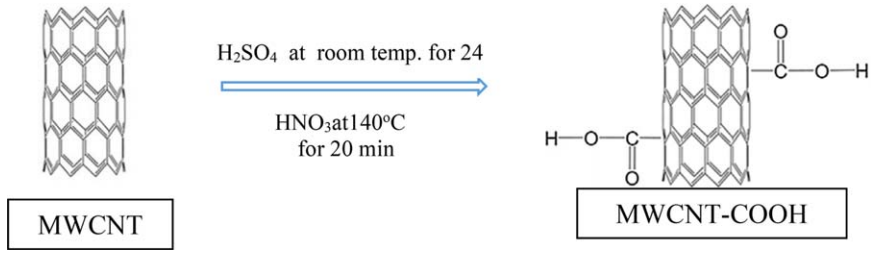

SCH. 1. Preparation of MWCNT-COOH.

adhesion. Polyurethane materials are also widely used in the medical field, owing to their excellent mechanical properties and biocompatibility. Particularly, they display excellent protein adsorption resistance.

Moreover, nano-vanadium pentoxide was studied as an additive in paint to prevent marine biofouling on its surfaces [9]. Nanopaint was developed by Yong et al. [10], by incorporating ZnO nanoparticles in alkyd resin matrix for antibiofouling applications.

Pristine MWCNTs have a hydrophobic surface and poor dispersion stability, and to improve dispersibility, pretreatment is needed. It has also been reported that CNTs, with an increased number of functional groups following oxidative treatment, lead to fine dispersion of nanoparticles on the CNTs surface [11].

However, Carl et al. [12] studied nanofillers such as TiO_2 and un-FCNTs incorporated in polydimethylsiloxane (PDMS) matrix. The results showed that the CNTs is ineffective in improving antifouling and foul-release properties against plant grades of the mussel *Mytilusgalloprovincialis*, when compared to the nanofiller (TiO_2).

Functionalization of CNTs with organic chains or functional groups will not only improve their dispersion, but also facilitate the interactions between them and the polymer matrix [13]. In addition, ionization radiations such as gamma rays and electron beams have also been used to modify MWCNTs. Gamma irradiation destroys the unstable five-and seven-membered rings of the CNTs to generate more defects, which provide sites for subsequent oxidization by acids to form more functional groups on the CNT surfaces [14]. Moreover, gamma irradiation can be easily controlled and prevent impurities in the materials [15]. Safibonab et al. [14] and other researchers [16] have estimated the effect of γ-rays on the surface area of MWCNTs and have showed larger surface area and pore volume with carbonyl functional groups in MWCNTs irradiated at 100 kGy.

Few studies [1, 17–19] have been carried out to examine the antifouling behavior of polymer nanoparticles on different objects, but no published data is available in case of γ-irradiated polyurethane/FMWCNT nanocomposites coating for wood ships. The current study is aiming to focus on developing γ-irradiated polyurethane/functionalized multiwall CNTs nanocomposites, as a coating for wood, having excellent mechanical, good adhesion, and antimicrobial properties (antifouling). Microalgae (*Chlorella vulgaris*) challenged the antifouling ability. Functionalization of MWCNT with carboxylic groups has been chosen before irradiation to combine the characteristics of functionalization and irradiation together.

EXPERIMENTAL

Materials

Toluene-2,4-diisocyanate TDI (Fluka, Germany). Polyethylene glycol (PEG) Mn =600 g/mol (Fluka, Germany), OH functionality = 2.0. Methyl ethyl ketone (MEK), Butanone, ADWIC Co. MWCNT, with average diameter of 10–50 nm and length of 1–25 mm, obtained from the Carbon Nanotube, Incheon, Korea. Purity of the received MWCNT is 93%. MWCNT was washed with dimethyl sulfoxide prior to use. *Acacia* wood, derived from the trees and shrubs of the *Acacia* genus native to Australia but also found in Asia, the Pacific Islands, Africa, and parts of the Americas. *Acacia* wood is smooth to touch, particularly if it has been polished. The Latin name for *Acacia* wood found in Egypt is *Acacia laeta*.

Functionalization of MWCNT

Carboxylic acid groups were created on the surface of MWCNTs through oxidation by nitric/sulfuric acid treatment [20]. Pristine (600 mg) of CNT was soaked in 60 mL of concentrated H_2SO_4 acid, stirring at room temperature for 24 h, and then sonicated for 1 h. After that, 20 mL of HNO_3 (70%) was added to the preceding mixture, while stirring at 140°C for 20 min. The resultant mixture was then diluted with distilled water, centrifuged at 4,000 rpm, and washed with deionized water several times [21]. Excess water was then decanted, and then the FMWCNTs were vacuum-filtered until the pH of the filtrate became neutral. The filtered solid was dried in a vacuum oven for 24 h at 50°C. The schematic for the preparation of MWCNT–COOH is shown in Scheme 1.

Gamma Irradiation

Irradiation was carried out using Cobalt-60 gamma cell source (made in Canada) installed at the National Center for Radiation Research and Technology, Egyptian Atomic

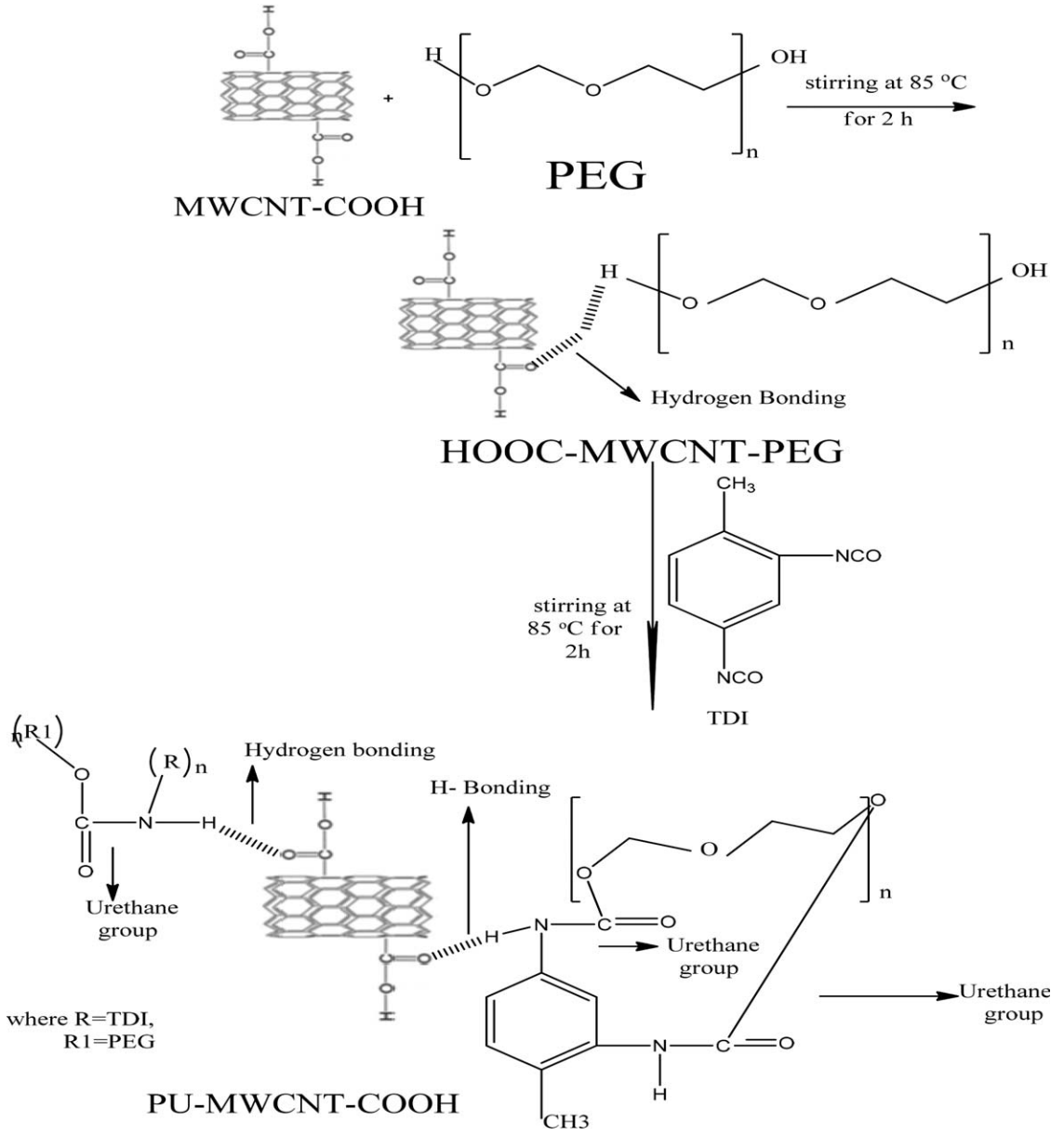

SCH. 2. Preparation of MWCNT-COOH with polyurethane.

Energy Authority, Cairo, Egypt. The direct radiation was used to induce the curing process of FMWCNT at 25–150 kGy, at a dose rate of 1.73 kGy/h.

Preparation of PU/MWCNT and PU/FMWCNT Nanocomposites

PU/MWCNT and PU/FMWCNT nanocomposites are prepared using *in situ* polymerization method. Various weights (0.05, 0.1, and 0.2%) of MWCNT and γ-irradiated FMWCNT are swelled in PEG containing MEK and stirred for 2 h at 85°C. Thereafter, the PEG/MWCNT mixture is stirred vigorously for 2 h at 85°C with the calculated amount of TDI as shown in Scheme 2. The obtained nanocomposites were then painted on wooden samples

Preparation of Coated Samples

The PU/MWCNT and PU/FMWCNT nanocomposites (≈14 g for each bar) was used to coat a rectangular bar of *Acacia* wood (1 × 2 × 5 cm). *Acacia* wood is smooth, so no sanding was needed. Each rectangular bar was painted all over manually using a coating knife. Thereafter, the bar was left hanged in the air for 24 h, and then it was dried in an oven at 40°C. To ensure complete removal of solvents, the sample was weighted at several time intervals until a constant weight was reached.

Characterization and Measurements of Coated Samples

Fourier Transform Infrared Spectroscopy (FTIR). Attenuated total reflectance Fourier transform infrared

 DOI 10.1002/pc

spectroscopy (ATR-FTIR) was used to investigate acid treatment on the surface MWCNT and the interaction between MWCNT and the PU matrix. The Vertex 70 FTIR spectrometer was equipped with HYPERION^{TM} series microscope, Bruker Optik GmbH, Ettlingen, Germany, over the 4,000–500 cm^{-1} range, at a resolution of 4 cm^{-1}. Software OPUS 6.0 (BRUKER) was used for data processing, whose baseline was corrected by the rubber band method, with CO_2 bands excluded.

Transmission Electron Microscopy (TEM). TEM was used to describe the modification of nanoparticles. TEM is performed usingTEM-1230, with an accelerating voltage of 100 KV (JEOL, Japan).

Field Emission Scanning Electron Microscopy (FESEM). The particle size distribution and surface morphology of nanoparticles embedded in polymer nanocomposites were examined using a high resolution scanning electron microscope (FESEM, Quanta FEG250 INSPECTS Company, Philips, Holland). The samples were sprayed with a thin layer of gold before being scanned.

Scanning Electron Microscopy. SEM studies of coated wooden samples were carried out by JEOLJSM-5400 high resolution (Japan), at 20 MA and 15 KV. The samples film was cut and sputter-coated with gold using a microscope sputter coater, viewed under the microscope.

Mechanical Measurements. *Hardness.* Hardness of the coated wooden samples was measured using Wolff-Wiborn pencil hardness tester, according to ASTM D 3,363 [22]. The following scale of hardness was used:

$$6B - 5B - 4B - 3B - 2B - B - HB - F - H - 2H - 3H - 4H - 5H - 6H$$

Softer Harder

Adhesion. The apparatus used to measure coating adhesion consists of a cutting tool with six blades, cutting distance of a 1 mm tape, a magnifying glass, and a brush. The cross-cut test procedure was performed according to ASTM D 3,359 – 97 [23].

Bending. Bending test of cured coating was done by Sheen Instruments, England, according to ASTM D 522-93a [24], where the elongation tests equipment consisted of rods including cylindrical mandrels of different diameters. The cured coating panels were bent over cylindrical mandrels of 2 mm in diameter, and resistance of the coating to cracking was determined.

Water Absorbance. The water absorbance properties of coated wooden samples were estimated by immersing each wooden sample (W_o) in a beaker containing water from the river Nile at 25°C, for 24 h. The sample was then removed from the beaker and quickly placed between two pieces of dry blotting paper, to remove residual water on the surface. Then it was reweighed quickly (W), and the percentage of water absorbance was calculated according to the following equation:

$$\text{Water absorbance}\,(\%) = \{(\mathbb{W} - \mathbb{W}o)|\mathbb{W}o\} \times 100 \qquad (1)$$

Algal Culture and Media. The *C. vulgaris* (green algae grown in fresh water) used in this study was cultivated in BG-11 medium, consisting of 1.50 g/L $NaNO_3$, 0.04 g/L K_2HPO_4, 0.075 g/L $MgSO_4 \cdot 7H_2O$, 0.036 g/L $CaCl_2 \cdot 2H_2O$, 0.006 g/L citric acid, 0.006 g/L Fe ammonium citrate, 0.02 g/L Na_2CO_3,0.001 g/L Na-EDTA, and 1 mL of trace metal solution per liter. The trace metal solution contained 2.86 g/L H_3BO_3, 1.81 g/L $MnCl_2 \cdot 4H_2O$, 0.222 g/L $ZnSO_4 \cdot 7H_2O$, 0.39 g/L $Na_2MoO_4 \cdot 2H_2O$, 0.079 g/L $CuSO_4 \cdot 5H_2O$, and 0.0494 g/L Co $(NO_3)_2 \cdot 6H2O$. It was grown in 1-L glass flasks under continuous illumination 40 $\mu E\ m^{-2}\ s^{-1}$, with constant air bubbling at 25°C. The coated wooden samples were immersed in the algal culture for 21 days and then picked up, dried, and examined using a SEM.

The water used in the water absorbance test and antifouling test was taken from the surface layer water of the river Nile at a depth of 50 cm.

Growth Determination. The growth rate of cultures on the surface of coated wooden samples was determined by measuring the optical density, (SPECORD 210 plus, 0.5; 1; 2; and 4 nm, double-beam spectrophotometer, Analytik Jena, Germany), in which 3 mL was drawn from the culture flask at a regular interval of 5 days. The measurements were taken at 680 nm to determine the growth of the culture.

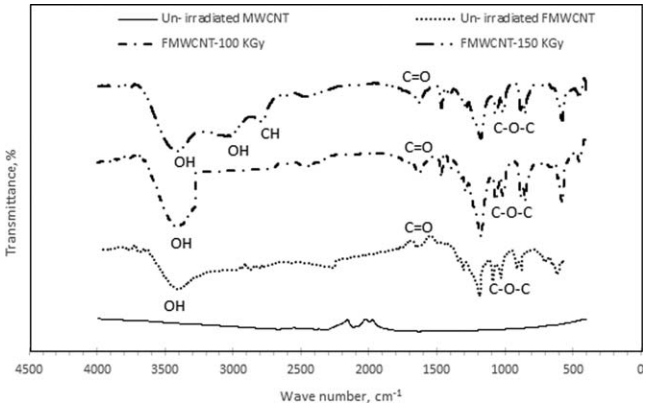

FIG. 1. FITR spectra of the pristine MWCNT, unirradiated FMWCNT, FMWCNT/γ-irradiated at 100 kGy and FMWCNT/γ-irradiated at 150 kGy.

RESULTS AND DISCUSSION

Fourier Transform Infrared Spectroscopy

The FTIR spectra of pristine MWCNT, un-irradiated FMWCNT and γ-irradiated FMWCNT at 100 and 150

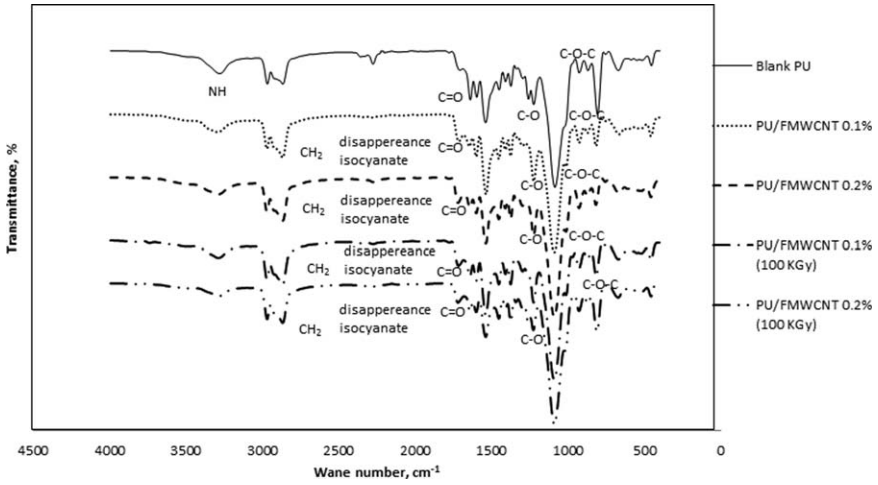

FIG. 2. FITR spectra of neat PU, PU/ unirradiated 0.1% FMWCNT, PU/unirradiated 0.2% FMWCNT, PU/irradiated at 100 kGy 0.1% FMWCNT, PU/irradiated at 100 kGy 0.2% FMWCNT.

KGy are shown in (Fig. 1). As shown in the figure after acid treatment, a peak at 3,415 cm^{-1} can be seen, corresponding to the O—H stretching of the carboxylic acid group. In addition, the absorption peak around 1,626 cm^{-1} is attributed to the stretching vibrations of the acid carbonyl (C═O) domain of the carboxylic acid groups appearing on the MWCNT surface [25].The results indicate that the carboxylic acid group is successfully grafted to the surface of MWCNT. The peak at 1,067 cm^{-1} assigned to the vibration of the C—O bond in primary alcohol, which appears on the MWCNT surface. The strong absorbance peak around 1,171 cm^{-1} is limited to the C—O stretching mode.

The spectrum of FMWCNT irradiated at 100 KGy indicates an intensive peak at the wave number of 3,401 and 1,700 cm^{-1} and this refers to a strong hydrogen bond, which subsequently means an increase in degree of the crosslinking. Furthermore, the spectrum of FMWCNT irradiated at 100 KGy is relatively similar that of unirradiated FMWCNT. However, the spectrum of FMWCNT irradiated at 150 KGy has a different peaks at 2,783 and 3,055 cm^{-1} confirms the development of defective structures in the irradiated FMWCNTs with the absorbed dose of 150 kGy [14].

The FTIR spectra for neat PU, PU/unirradiated FMWCNT and PU/γ-irradiated FMWCNT nanocomposites are presented in (Fig. 2). The FTIR spectra were used to investigate the interaction between —COOH modified MWCNT and the PU matrix. For the FTIR spectrum of PU/FMWCNT nanocomposites, it is observed that the band around 3,280–3,296 cm^{-1} is an overlap of the —NH group stretching of urethane linkage and —OH stretching of MWCNT–COOH [26]. The absorption peaks at around 1,719 and 1,645 cm^{-1} are due to >C═O groups present in the urethane linkage (—HN—COO—) of the PU matrix, respectively. Several peaks appeared for the PU/FMWCNT, such as the peaks around 2,943 and 2,867 cm^{-1} attributed to the asymmetrical and symmetrical stretching vibrations of the C—H bonds of methylene groups in the alkane chain [27]. The peak at around 1,092 cm^{-1} is due to the C—O stretching characterized for the ether linkage (C—O—C) [28], and the peak at around 1,227 cm^{-1} can be attributed to the C—O stretching. It is noticed that these absorbance peaks remarkably increase by increasing the wt% of loaded FMWCNT (0, 0.1, 0.2), due to the hydrogen bond between O═C═O of the —COOH group on MWCNT and the —NH group of the PU matrix. Moreover, the magnitude of hydrogen bond increases with increasing FMWNT concentration. These peaks proved that the interfacial interaction between FMWCNT and PU matrix observably increases as the wt% of loaded FMWCNT increases [29].

Furthermore, as seen in Table 1, the carbonyl group in FMWCNT, PU, and PU/FMWCNT has different absorption peaks and is shifted to higher frequencies. There is also a difference in the shift frequencies between unirradiated and irradiated samples.

Transmission Electron Microscopy

Pristine MWCNT and MWCNT-COOH were described using TEM, as presented in (Fig. 3a and b).Pristine MWCNT exhibited a comparatively smooth and clean surface due to its complete lattice structure of carbon network. However, the walls of MWCNT–COOH (Fig. 3b) appeared to be very rough, due to the attachment of carboxylic acid groups on MWCNTs' surface.

Dispersion of FMWCNT in PU

An efficient method to realize uniform dispersion of CNT in a thermosetting polymer is *in situ* polymerization. In this method, CNT was mixed with monomers in the presence of a solvent, and then these monomers were polymerized with a hardener or curing agents at an elevated temperature [30].

 DOI 10.1002/pc

TABLE 1. Infrared characteristic absorption peaks for MWCNT, FMWCNT, and PU/FMWCNT 0.1, 0.2% (irradiated and unirradiated).

Main assignments of absorption beaks	MWCNT	FMWCNT	FMWCNT 100 KGy	FMWCNT 150 KGy	PU Blank	PU/FMWCNT 0.1% Unirradiated	PU/FMWCNT 0.2% unirradiated	PU/FMWCNT 0.1% 100 KGy	PU/FMWCNT 0.2% 100 KGy
v (NH) (cm^{-1})	—	—	—	—	3,281	3,296	3,294	2,991	3,286
v (OH) (cm^{-1})	—	3,415	3,401	3,408	—				
				3,055					
v_s (CH_2) (cm^{-1})	—	—	—	—	2,868	2,869	2,869	2,869	2,868
v_{as} (CH_2) (cm^{-1})	—	—	—	—	2,969	2,972	2,972	2,972	2,970
v (C═O) (cm^{-1})	—	1,627	1,626	1,628	1,641	1,715	1,720	1,717	1,721
δ_{as} (CH) (cm^{-1})		—	—	2,783					
v_s (C─O─C) (cm^{-1})	—	1,171	1,183	1,176	1,086	1,088	1,088	1,088	1,088

v, stretching vibration; v_s, symmetric stretching vibration; v_{as}, asymmetric stretching vibration; δ_{as}, asymmetric bending vibration.

FESEM was used to confirm the dispersion of MWCNTs in the PU matrix. (Fig. 4a–d) shows the FESEM images of the studied nanocomposites: (a) PU/unirradiated FMWCNT 0.1 wt%, (b) PU/unirradiated FMWCNT 0.2 wt%, (c) PU/FMWCNT 0.1 wt% irradiated at 100 KGy and (d) PU/FMWCNT 0.2 wt% irradiated at 100 KGy, respectively.

Homogeneous dispersion of FMWCNT in the PU matrix is shown in (Fig. 4a), and there is no aggregation phenomenon. This means that there is strong interfacial adhesion between FMWCNTs and PU. This phenomenon can be explained in terms of improved interfacial interaction between the MWCNT and PU (that is, CNT-OH) by forming covalent bonds, and it should lead to improved disagglomeration of the nanotube bundles and good dispersibility of MWCNTs in the PU matrix. It was attributed to the increase in polarity of the MWCNTs by the functional groups and interaction of the ─OH group of CNTs with the isocyanate (─NCO─) group of the PU matrix [31–33]. Increasing the content of FMWCNT to 0.2 wt% leads to the conductive network structure becoming more apparent and dense, which means no homogeneous dispersion of the FMWCNTs happens in the PU matrix, as shown in (Fig. 3b).

However, for irradiated 0.1 wt% FMWCNT (Fig. 4c) shows a smooth morphology, better dispersion, and more uniformity in the matrix than unirradiated FMWCNT. Finally, for irradiated 0.2 wt% FMWCNTs, it appears from (Fig. 4d) that the dispersion level of γ-irradiated FMWCNTs is continuous in the polymer phase. Furthermore, no agglomerates are seen in these nanocomposites as compared with unirradiated FMWCNT having the same content. The reason behind the change in the nanocomposites' morphology between unirradiated and irradiated samples is attributed to the formation of radiation crosslinking network among the PU chains and γ-FMWCNT [34].

Mechanical Properties of PU/FMWCNT for Coating Wooden Samples

The major advantage of *in situ* polymerization is that covalent bonding can be formed between the FCNTs and the polymer matrix, resulting in much improved mechanical properties. The mechanical properties of wooden samples coated with polyurethane elastomers loaded with different concentrations of MWCNT and γ-irradiated FMWCNT are shown in Table 2. Average values with standard deviation were reported from four measurements taken for each composition.

Initially, it has been observed that the wooden sample coated with neat PU and those coated with PU/MWCNT are less hard than those coated with PU/FMWCNT. In addition, the hardness value increases by increasing the concentration of FMWCNT for all the cured coated samples. Increased hardness values result from good dispersion of

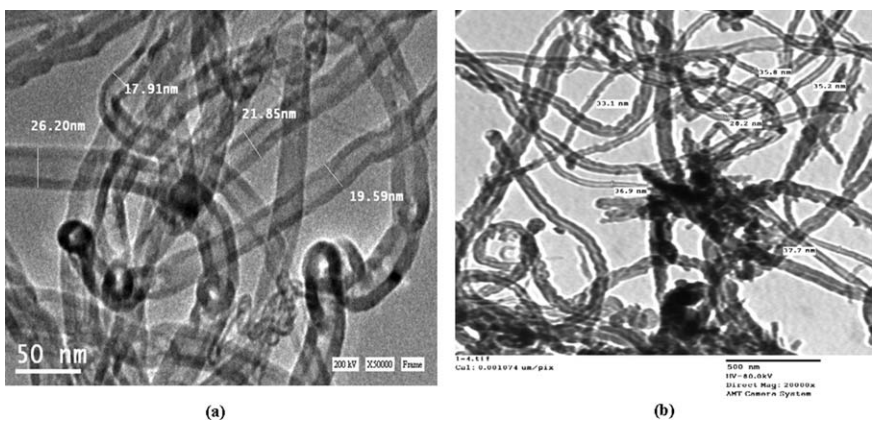

FIG. 3. TEM images of (a) pristine of MWCNT and (b) MWCNT-COOH.

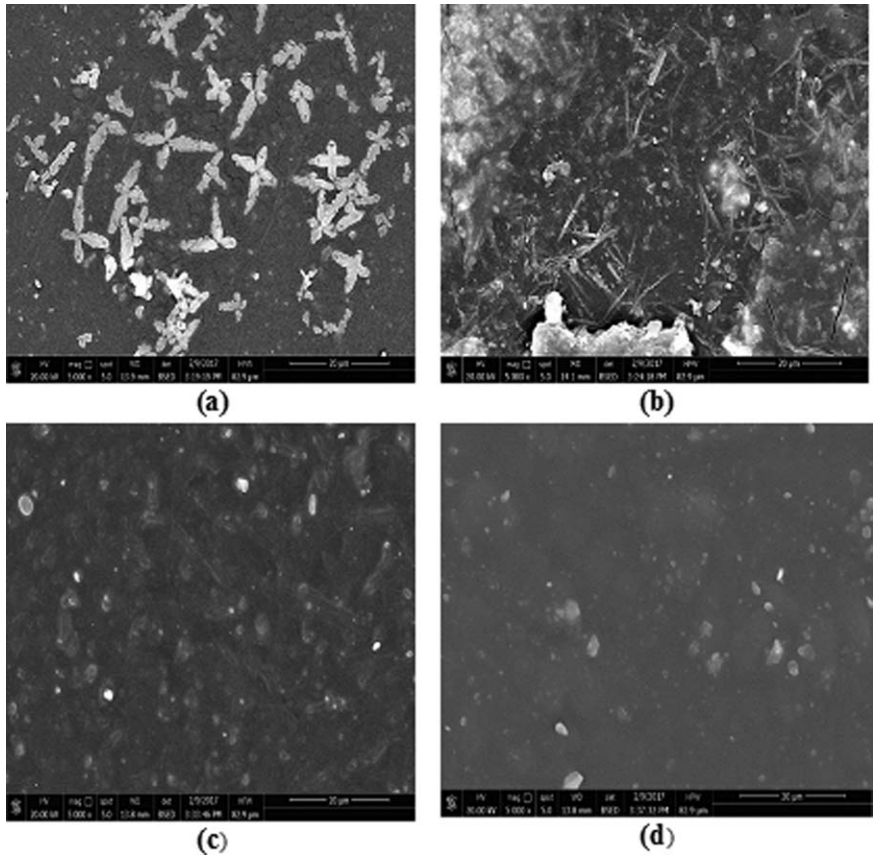

FIG. 4. FESEM images of the surface-fractures: (a) PU/unirradiated FMWCNT 0.1 wt%, (b) PU/unirradiated FMWCNT 0.2%, (c) 100 KGy irradiated PU/FMWCNT 0.1%, and (d) 100 KGy irradiated PU/FMWCNT 0.2%.

FMWCNT in the PU matrix, as shown in FESEM, as well as increasing the hydrogen bond formation due to functionalization with carboxylic groups. Additionally, increasing irradiation doses from zero up to 100 kGy leads to increasing the hardness values of the nanocomposites. This increase may be due to the formation of a high degree of

TABLE 2. Mechanical properties of the wooden samples coated with neat PU, PU/MWCNT, and PU/FMWCNT unirradiated and γ-irradiated (25–150 kGy) at different concentrations.

Concentration (%)	Irradiation doses (kGy)	Hardness*	Adhesion**
Blank PU	0	1H ± 0.05H	1B ± 0.025
PU/0.05% MWCNT	0	1H ± 0.05H	1B ± 0.03
PU/0.05% FMWCNT	0	2H ± 0.1H	1B ± 0.05B
	25	2H ± 0.1H	2B ± 0.025
	50	3H ± 0.02H	3B ± 0.1
	100	4H ± 0.05H	4B ± 0.05
	150	2H ± 0.05H	2B ± 0.1
PU/0.1% MWCNT	0	2H ± 0.04H	1B ± 0.03B
PU/0.1% FMWCNT	0	3H ± 0.02H	2B ± 0.025
	25	4H ± 0.019H	3B ± 0.025
	50	5H ± 0.05H	4B ± 0.1
	100	6H ± 0.05H	5B ± 0.1
	150	3H ± 0.05H	3B ± 0.05
PU/0.2% MWCNT	0	2H ± 0.05H	2B ± 0.02
PU/0.2% FMWCNT	0	3H ± 0.05H	3B ± 0.01
	25	5H ± 0.1H	4B ± 0.025
	50	6H ± 0.05H	4B ± 0.15
	100	7H ± 0.05H	5B ± 0.1
	150	4H±0.1H	3B ± 0.1

 DOI 10.1002/pc

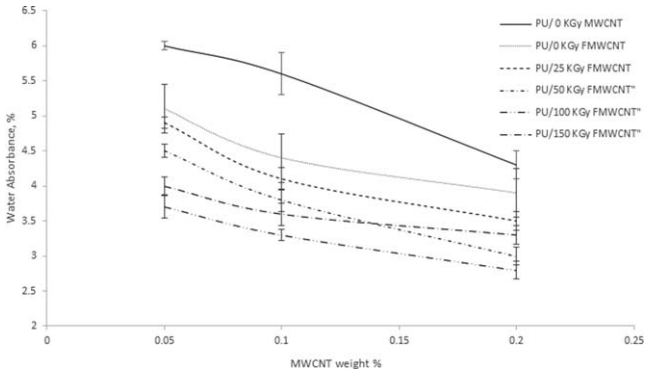

FIG. 5. Water absorbance % for PU/MWCNT, PU/unirradiated FMWCNT, PU/γ-irradiated FMWCNT nanocomposites at different does for different concentration. [Color figure can be viewed at wileyonlinelibrary.com]

crosslinking induced by irradiation treatment. Furthermore, modification of FMWCNT by irradiation process lead to an improvement in the hydrogen bond formed between FMWCNT and PU chains, increasing the hardness of the cured samples. However, the decrease in hardness for all concentrations of PU/FMWCNT at irradiation dose 150 kGy is a result of the radiation process that destroyed or retreated the structure of FMWCNT as shown by the FTIR. From all the previous results, it is concluded that all the polyurethane coated samples show good hardness.

Secondly, Table 2 has shown that the adhesion of wooden samples coated with PU/FMWCNT nanocomposites is better than that of those coated with PU/MWCNT nanocomposites and neat PU and increased by increasing the concentrations of FMWCNT for all the coated samples. Likewise, increasing the irradiation dose from zero to 100 kGy improved adhesion in all wooden samples coated with PU/irradiated FMWCNT. At an irradiation dose of 150 kGy, a decrease in the adhesion for all concentrations of FMWCNT was also noticed. All samples of formulation showed excellent adhesion to wood, while the best adhesion resulted from the interaction of coated polyurethane on wood.

Finally, all the cured samples were successfully passed the bending test, succeeding in passing the 2 mm diameter. This means that the flexibility of all cured samples is very good, which is due to the high elasticity of polyurethane.

Water Absorbance

Water absorption properties of PU films are important, importance of this phenomena' to avoid hydrolytic degradation of the films. The water absorbance % of uncoated wood and wooden sample coated with neat PU is 20 ± 1.7 and 5.9 ± 0.16, respectively. The water absorbance % of PU/MWCNT, PU/unirradiated FWMCNT and PU/γ-irradiated FWMCNT of different concentrations is illustrated in (Fig. 5). Average values with standard deviation were reported from four measurements taken for each composition. The figure shows that PU/unirradiated FMWCNT has lower values of water uptake than PU/MWCNT samples. As well as, PU/γ-irradiated FMWCNT formulations showed a significant decrease in water absorbance, which gives the samples higher hydrophobicity than the samples uncoated, coated with neat PU and those coated with PU/MWCNT. Moreover, it is observed that water absorbance decreases with increasing the irradiation to 100 KGy for all FMWCNT concentrations, due to induced crosslinking during the irradiation process. However, water absorbance slightly increases in the samples coated with PU/irradiated FMWCNT at 150 KGy. This increase may be attributed to the degradation effect of γ-irradiation on FWMCNT, which has destroyed the nanostructure of carbons, leading to defects in the structure of FMWCNT [14]. It can also be seen that the water uptake decreases by increasing the content of FMWCNT (0.05, 0.1, and 0.2 wt%), due to the hydrogen bond formation and good dispersion shown by FESEM.

It can be concluded that PU/γ-irradiated FWMCNT samples, which show lower water uptake, have higher crosslink density than those coated with PU/unirradiated FWMCNT and neat PU. The higher crosslink density could retard the diffusion of water molecules into PU films. Furthermore, the higher crosslink density led to restriction in the polymer chain mobility and a decrease in the hydrolytic degradation of PU coating [35]. Therefore, PU/γ-irradiated FWMCNT samples up to 100 KGy, which have the highest crosslinking, are better for coating ship hulls.

In spite of the possible hazards of isocyanates that can happen through direct exposure (inhalation, skin contact, eye contact, or swallowing), it is known that after curing, polyurethane paints contain no free isocyanates, which has been confirmed by FTIR spectra of the polyurethane, where the peak assigned for the toluene di-isocyanate disappeared. Therefore, no unreacted species are present. In addition, fully reacting polyurethane polymer is chemically inert. From the above results, it can be concluded that it is safe to use these nanocomposites and any polyurethane coating prepared with a similar technique for coating ship hulls.

Antifouling Properties

Growth (O.D.) of the green microalgae *C. vulgaris* (alone) and in the presence of wood samples coated by neat PU,PU/MWCNT, PU/unirradiated FMWCNT, and PU/irradiated FMWCNT at (25, 50, 100, and 150 kGy) for all concentrations of MWCNT and FMWCN, is shown in Table 3. Average values with standard deviation were reported from four measurements values taken for each composition. Immersion of coated samples in the algae culture revealed that the growth of *C. vulgaris* (alone) is higher than its growth in the presence of coated wood samples. On the other hand, the wood samples coated with PU/γ-irradiated FMWCNT at 100 kGy for all concentrations exhibit the best *C. vulgaris* growth inhibition. It was also observed that increasing the concentration of FMWCNT decreases the growth of *C. vulgaris* to

TABLE 3. Growth of green microalgae (*C. vulgaris*) in the liquid growth medium for neat PU, PU/MWCNT, and PU/FMWCNT unirradiated and irradiated at different concentrations.

Concentration (%)	Radiation dose (KGy)	Days and spectrum values				
		1	5	10	15	20
C. vulgaris	0	0.1156 ± 0.0004	0.3850 ± 0.0004	0.7922 ± 0.0001	0.8967 ± 0.0002	1.5249 ± 0.0005
Blank PU	0	0.0308 ± 0.002	0.5560 ± 0.002	0.8932 ± 0.0005	1.0390 ± 0.0005	1.3479 ± 0.0005
0.05% MWCNT	0	1.2785 ± 0.00012	1.0787 ± 0.0006	0.9453 ± 0.00005	0.7132 ± 0.0038	0.0945 ± 0.00012
0.0.5% FMWCNT	0	0.0843 ± 0.0002	0.6130 ± 0.0003	0.8354 ± 0.0002	0.9787 ± 0.0004	1.1785 ± 0.0002
	25	0.1676 ± 0.0003	0.4270 ± 0.0003	0.7201 ± 0.0002	0.8720 ± 0.0002	1.2352 ± 0.0003
	50	0.1408 ± 0.0003	0.2700 ± 0.0002	0.5957 ± 0.0003	0.7000 ± 0.0003	0.9097 ± 0.0003
	100	0.2339 ± 0.0002	0.4690 ± 0.0003	0.7800 ± 0.0002	0.9151 ± 0.0001	1.2017 ± 0.38
	150	0.1481 ± 0.0003	0.4360 ± 0.0002	0.7148 ± 0.0002	0.8555 ± 0.0003	1.1706 ± 0.0003
0.1% MWCNT	0	1.3480 ± 0.0001	0.8833 ± 0.0005	0.7785 ± 0.0002	0.5450 ± 0.0003	0.1686 ± 0.00012
0.1% FMWCNT	0	0.1580 ± 0.0003	0.4450 ± 0.0007	0.6783 ± 0.0004	0.7832 ± 0.0005	1.1480 ± 0.0001
	25	0.1685 ± 0.0003	0.4430 ± 0.001	0.7486 ± 0.0002	0.8572 ± 0.0001	1.0794 ± 0.0007
	50	0.1878 ± 0.0003	0.4710 ± 0.001	0.8328 ± 0.00015	0.9649 ± 0.0002	1.1782 ± 0.05
	100	0.0735 ± 0.0002	0.2530 ± 0.0003	0.6039 ± 0.0002	0.7028 ± 0.0002	0.9918 ± 0.0002
	150	0.1697 ± 0.0002	0.4730 ± 0.0003	0.8741 ± 0.0005	0.9968 ± 0.0002	1.4102 ± 0.0003
0.2% MWCNT	0	0.1646 ± 0.0002	0.4850 ± 0.0001	0.9061 ± 0.00009	1.0483 ± 0.0003	1.4412 ± 0.0002
0.2% FMWCNT	0	0.1546 ± 0.0002	0.3850 ± 0.0003	0.8062 ± 0.0003	0.9383 ± 0.0003	1.3412 ± 0.0001
	25	0.2682 ± 0.0002	0.5620 ± 0.05	0.8262 ± 0.0001	0.9415 ± 0.0002	1.1012 ± 0.0004
	50	0.1474 ± 0.0001	0.3890 ± 0.0002	0.7519 ± 0.0003	0.8797 ± 0.005	1.1667 ± 0.0003
	100	0.1024 ± 0.0001	0.4470 ± 0.0001	0.7704 ± 0.0003	0.8583 ± 0.0003	1.1955 ± 0.0004
	150	0.1637 ± 0.1	0.5170 ± 0.0003	0.9810 ± 0.0003	1.1593 ± 0.0002	1.4677 ± 0.0004

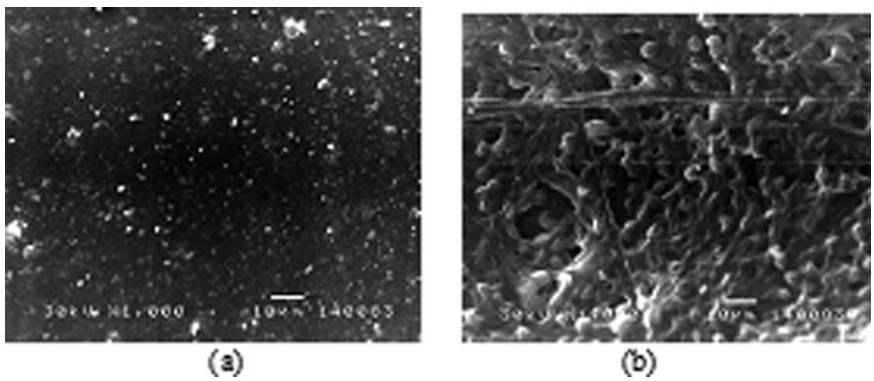

FIG. 6. SEM images for the effect of algae growth on (a) uncoated wood without algae and (b) wood coated with neat PU.

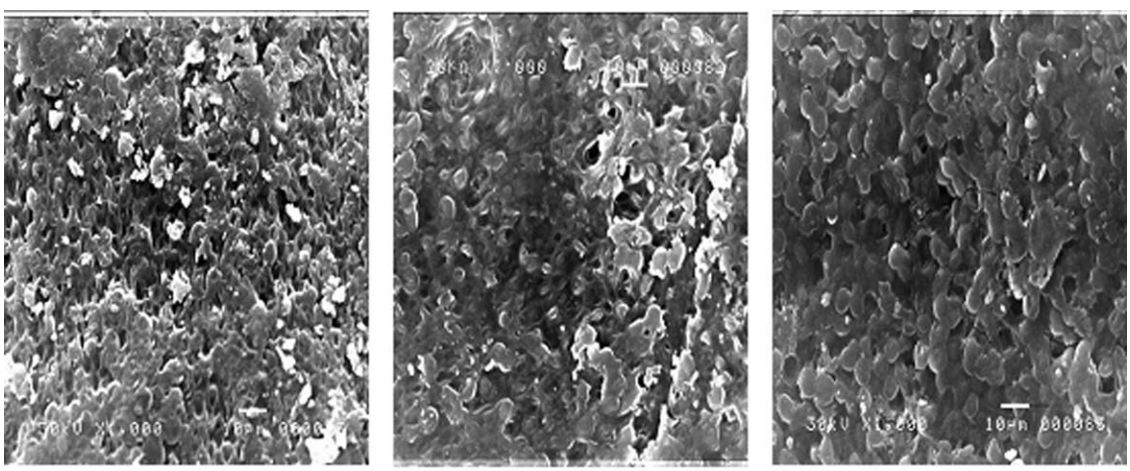

FIG. 7. SEM images for the effect of algae growth on (a) PU/0.05% MWCNT, (b) PU/0.1% MWCNT, and (c) PU/0.2% MWCNT. [Color figure can be viewed at wileyonlinelibrary.com]

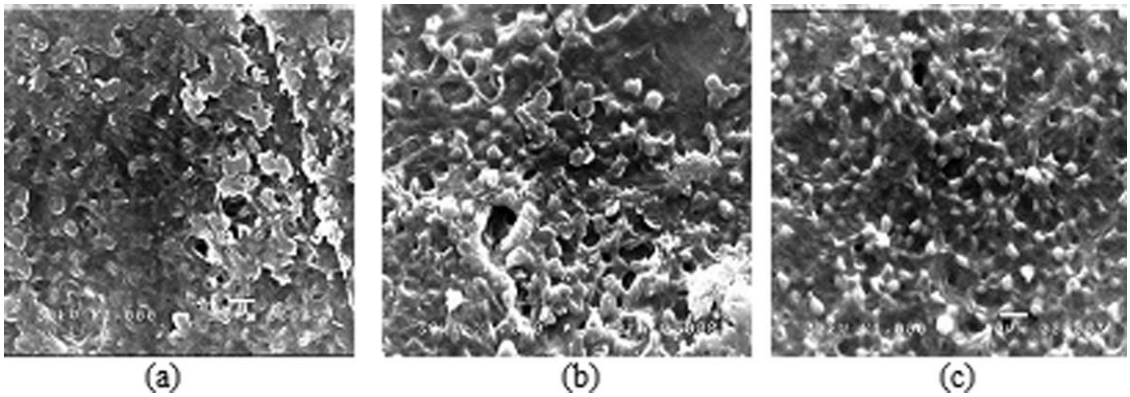

FIG. 8. SEM images for the effect of algae growth on (a) PU/0.05% FMWCNT unirradiared, (b) PU/0.05% γ-FMWCNT at 100 kGy, and (c): PU/0.05% γ-FMWCNT at 150 kGy.

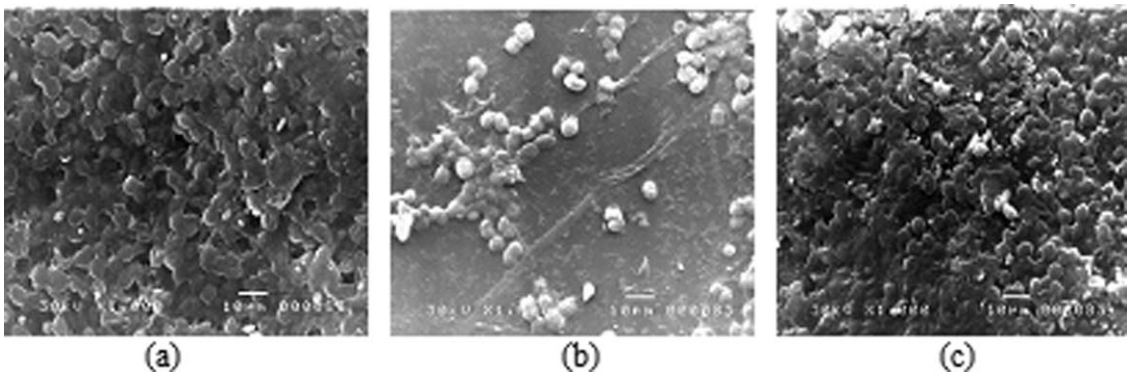

FIG. 9. SEM images for the effect of algae growth on (a) PU/0.1% FMWCNT unirradiared, (b): PU/0.1% γ-FMWCNT at 100 kGy, and (c): PU/0.1% γ-FMWCNT at 150 kGy.

100 kGy. However, increasing the irradiation dose to above 100 kGy (150 kGy) relatively increases the growth of *C. vulgaris*, due to the degradation effect of the FMWCNT matrix. From the results obtained from the SEM seen in (Figs. 6–10) the images revealed that the most efficient treatment for wood surface was coating it by PU/0.1 wt% FMWCNT and PU/0.2 wt% FMWCNT irradiated at 100 kGy. The images show that treatment inhibited the growth of algae on the surface of coated wood. All results of characterization and measurements of wooden samples and of antifouling revealed that the most efficient samples were those coated with 0.1 wt% and 0.2 wt% of PU/FMWCNT γ-irradiated at 100 kGy.

The previous results of the present study were confirmed by other investigators as follows:

Yong et al. [10] developed ZnO nano-paint for prevention of marine biofouling, while Carl et al. [12] enhanced fouling release (FR) coatings that minimize the adhesion strength of fouling organisms by incorporating nano-TiO in PDMS matrices instead of CNT. However, Zhang et al.

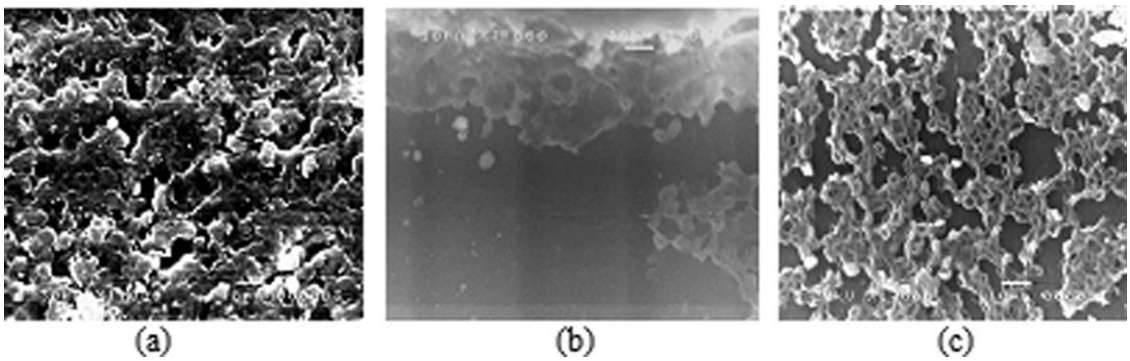

FIG. 10. SEM images for the effect of algae growth on (a): PU/0.2% FMWCNT unirradiared, (b) PU/0.2% γ-FMWCNT at 100 kGy, and (c): PU/0.2% γ-FMWCNT at 150 kGy.

[36] used a type of polyurethane antifouling coating, and the results showed that polyurethane has good antiprotein adsorption properties and could be used as antifouling material, and that the best antifouling coating was that containing a hard segment content of polyurethane of 40%.

Diatoms fouling has also been studied as a component of adhered microbial films. Diatoms are primary colonizers of both antifouling and FR ship hull coatings [37, 38]. Zargiel et al. and Holland et al. [39, 40] found that adhesion of the three common fouling diatoms to polydimethylsiloxane elastomer (PDMSE) was stronger than that to glass. However, Gladis et al. [41] used green microalgae as a test organism of the genus *Stichococcus* to evaluate the anti-aglae activity of two biocides (thiazine and isothiazoline) and photocatalytic nanoparticles of ZnO (20–60 nm).The results have revealed that the herbicide thiazine did not kill the algae cells, while due to the multiple modes of action isothiazoline and photocatalytic nanoparticles activated with UV irradiation severely impacted all performance and structure parameters.

Bioadhesion and surface wettability are influenced by micro-scale topography. Appropriate nano-scale topographies have been shown to prevent cell attachment by prohibiting formation of focal contact [42, 43], while the green macroaglae (*Enteromorpha*) zoospores colonized (fouling) different surfaces, depending on the number of settlement cues. The majority of spores settled in the angle between the valley floor and side wall [44].

No investigators have previously used this combination between functionalization of MWCNT and gamma irradiation of it and combined it with polyurethane. Therefore, this antifouling coating is novel and was not mentioned in previous studies. From all the previous studies, it was clear that wooden samples coated with polyurethane supplemented with γ-irradiated FMWCNT can be used as excellent promising antifouling coating paints for ship hulls, especially when this coating substance is exposed to different doses of gamma irradiation, which increased the crosslinking and improved hydrogen bond formation between PU and FMWCNT.

CONCLUSIONS

- This set of experiments show the applicability of polyurethane/γ-irradiated FMWCNT FR coatings in ship hulls.
- A series of PU/γ-irradiated FMWCNT nanocomposites for various amounts (0.05, 0.1, and 0.2 wt%) of FMWCNT with different irradiation doses are prepared, and these nanocomposites are used for painting rectangular wood bars.
- The FTIR spectra proved the presence of acid treatment on the MWCNT surface, and there are strong interactions between the —COOH modified MWCNT and the PU matrix.
- From FESEM, a homogeneous dispersion of FMWCNT into the PU matrix at concentrations 0.1 and 0.2 wt% was seen. The irradiated samples were also smooth and had better dispersion than unirradiated samples. In addition to that, dispersion increases as the concentration of FMWCNT increases in the PU.
- Mechanical properties of the coated wood samples showed that the hardness increases significantly by increasing the concentration of FMWCNT in all samples. Moreover, increasing irradiation doses for FMWCNT leads to increase in the hardness values, and all samples showed improvement in adhesion strength up to 5B, with an increase in irradiation doses and in concentrations of FMWCNT. Furthermore, the cured samples of all formulations passed the 2 mm diameter, which means that coating samples passed the bending test successfully due to high elasticity of polyurethane.
- Water absorbance in coated wooden samples was less than that in uncoated wood, but in the coated samples loaded with γ-irradiated FMWCNT it has been found to be more than that in those unloaded ones. It also decreases by increasing the concentration of FMWCNT.
- The results of the mechanical properties coincided with the results of antifouling done using *C. vulgaris* as a test organism; that is, the most efficient antifouling coating samples were those of PU/γ-irradiated FMWCNT with concentrations 0.1 and 0.2 wt% at 100 kGy.
- All the results revealed excellent promising antifouling coating paints for ship hulls, especially when exposed to different doses of gamma irradiation, which increased the crosslinking and improved hydrogen bond formation between the PU and FMWCNT.

ACKNOWLEDGMENT

The authors would like to thank Prof. Dr. Hussein Amer for guidance, Dr. Issa Mohammed for allowing time to undergo measurements of the coating on special devices, and Prof. Sanaa Shanab (Department of Botany and Microbiology, Faculty of Science, Cairo University, Giza, Egypt) for providing the *Chlorella vulgaris* used in this study.

REFERENCES

1. L. Al-Naamani, S. Dobretsov, J. Dutta, and J.G. Burgess, *Chemosphere*, **168**, 408 (2017).
2. K.V. Thomas, and S. Brooks, *Biofouling*, **26**, 73 (2010).
3. L.D. Chambers, K.R. Stokes, F.C. Walsh, and R.J.K. Wood, *Surf. Coat. Technol.*, **201**, 3642 (2006).
4. S. Cao, J. Wang, H. Chen, and D. Chen, *Chin. Sci. Bull.*, **56**, 598 (2011).
5. A. Beigbeder, P. Degee, S.L. Conlan, R.J. Mutton, A.S. Clare, M.E. Pettitt, M.E. Callow, J.A. Callow, and P. Dubois, *Biofouling*, **24**, 291 (2008).
6. P. Majumdar, S. Stafslien, J. Daniels, and D.C. Webster, *J. Coat. Technol. Res.*, **4**, 131 (2007).
7. S. Sommer, A. Ekin, D.C. Webster, S.J. Stafslien, J. Daniels, L.J. VanderWal, S.E.M. Thompson, M.E. Callow, and J.A. Callow, *Biofouling*, **26**, 961 (2010).
8. J.B. Dai, X.Y. Zhang, J. Chao, and C.Y. Bai, *J. Coat. Technol. Res.*, **4**, 283 (2007).
9. F. Natalio, R. André, A.F. Hartog, B. Stoll, K.P. Jochum, R. Wever, and W. Tremel, *Nat. Nanotechnol.*, **7**, 530 (2012).

10. H.E. Yong, K. Krishnamoorthy, K. Tae, and S. Jae, *J. Ind. Eng. Chem.*, **29**, 39 (2015).
11. A. Orfanidi, M.K. Daletou, and S.G. Neophytides, *Appl. Catal. B*, **106**, 379 (2011).
12. C. Carl, A.J. Poole, M.J. Vucko, M.R. Williams, S. Whalan, and R. de Nys, *Biofouling*, **28**, 175 (2012).
13. G.-X. Chen, and H. Shimizu, *Polymer*, **49**, 943 (2008).
14. B. Safibonab, A. Reyhani, A.N. Golikand, S.Z. Mortazavi, S. Mirershadi, and M. Ghoranneviss, *Appl. Surf. Sci.*, **258**, 766 (2011).
15. M.R. Karim, C.J. Lee, A.M.S. Chowdhury, N. Nahar, and M.S. Lee, *Mater. Lett.*, **61**, 1688 (2007).
16. T. Murakami, M. Matsuda, S. Isozaki, K. Kisoda, and C. Itoh, Mater. Sci. Eng., 12016 (2015).
17. R. Wang, X. Song, T. Xiang, Q. Liu, B. Su, W. Zhao, and C. Zhao, *Carbohydr. Polym.*, **168**, 310 (2017).
18. S. Sathya, P.S. Murthy, A. Das, G.G. Sankar, S. Venkatnarayanan, R. Pandian, V.S. Sathyaseelan, V. Pandiyan, M. Doble, and V.P. Venugopalan, *Int. Biodeterior. Biodegradation*, **114**, 57 (2016).
19. H. Shi, H. Liu, S. Luan, D. Shi, S. Yan, C. Liu, R.K.Y. Li, J. Yin, *Compos. Sci. Technol.*, **6**, 19238 (2016).
20. V. Vatanpour, S.S. Madaeni, R. Moradian, S. Zinadini, and B. Astinchap, *J. Membr. Sci.*, **375**, 284 (2011).
21. N.A. Kumar, H.S. Ganapathy, J.S. Kim, Y.S. Jeong, and Y.T. Jeong, *Eur. Polym. J.*, **44**, 579 (2008).
22. ASTM Standard D3363-05. Standard Test Method for Film Hardness by Pencil Test. American Society for Testing Materials (ASTM International), West Conshohocken, PA, USA (2005).
23. ASTM StandardD3359 – 97, Method B. Book of Standards Volume: 06.01, Standard Test Methods for Measuring Adhesion by Tape Test. American Society for Testing Materials (ASTM International), West Conshohocken, PA, USA (1997).
24. ASTM Standard D 522 – 93a. Annual Book of ASTM Standards, Vol 06.01, Standard Test Methods for Mandrel Bend Test of Attached Organic Coatings. American Society for Testing Materials (ASTM International), West Conshohocken, PA, USA (2001).
25. H. Deka, N. Karak, R.D. Kalita, and A.K. Buragohain, *Carbon*, **48**, 2013 (2010).
26. A.K. Barick, and D.K. Tripathy, *Compos A*, **41**, 1471 (2010).
27. S. Yun, H. Im, and J. Kim, *Synth. Met.*, **161**, 1361 (2011).
28. J. Xiong, D. Zhou, Z. Zheng, X. Yang, and X. Wang, *Polymer*, **47**, 1763 (2006).
29. A.K. Barick, and D.K. Tripathy, *Mater. Sci. Eng. B*, **176**, 1435 (2011).
30. P. Ma, N.A. Siddiqui, G. Marom, and J. Kim, *Compos. A*, **41**, 1345 (2010).
31. S.A. Shokry, A.K. El Morsi, M.S. Sabaa, R.R. Mohamed, and H.E. El Sorogy, *Egypt. J. Pet.*, **24**, 145 (2015).
32. P. Cheng, J. Kim, and B.Z. Tang, *Compos. Sci. Technol.*, **67**, 2965 (2007).
33. F.H. Gojny, M.H.G. Wichmanna, U. Köpkeb, B. Fiedlera, K. Schulte, Compos. Sci. Technol. **64**, 2363 (2004).
34. B. Ghafoor, M.S. Mehmood, U. Shahid, M.A. Baluch, and T. Yasin, *Radiat. Phys. Chem.*, **125**, 145 (2016).
35. J. Yi, C. Huang, H. Zhuang, H. Gong, C. Zhang, R. Ren, and Y. Ma, *Prog. Org. Coat.*, **87**, 161 (2015).
36. Y. Zhang, Y. Qi, and Z. Zhang, *Prog. Org. Coat.*, **97**, 115 (2016).
37. T. Kemmitt, A.G. Young, and C. Depree, *Mater. Sci. Forum*, **700**, 227 (2012).
38. A.J. Scardino, E. Harvey, and R. De Nys, *Biofouling*, **22**, 55 (2006).
39. K.A. Zargiel, J.S. Coogan, and G.W. Swain, *Biofouling*, **27**, 955 (2011).
40. R. Holland, T.M. Dugdale, R. Wetherbee, A.B. Brennan, J.A. Finlay, J.A. Callow, and M.E. Callow, *Biofouling*, **20**, 323 (2004).
41. F. Gladis, A. Eggert, U. Karsten, and R. Schumann, *Biofouling*, **26**, 89 (2010).
42. P.J. Molino, E. Campbell, and R. Wetherbee, *Biofouling*, **25**, 685 (2009).
43. M.L. Carman, T.G. Estes, A.W. Feinberg, J.F. Schumacher, W. Wilkerson, L.H. Wilson, M.E. Callow, J.A. Callow, and A.B. Brennan, *Biofouling*, **22**, 11 (2006).
44. M.E. Callow, A.R. Jennings, A.B. Brennan, C.E. Seegert, A. Gibson, L. Wilson, A. Feinberg, R. Baney, and J.A. Callow, *Biofouling*, **18**, 229 (2002).